



Modelling and optimisation of bio-inspired synthesis of porous silica particles: estimation of kinetics and application to continuous reactors[☆]

Chinmay A. Shukla^a, Roja P. Moghadam^a, Amber Keegan^b, Siddharth V. Patwardhan^b, Vivek V. Ranade^{a,*}

^a Multiphase Reactors and Process Intensification Group Bernal Institute, University of Limerick, Ireland

^b Green Nanomaterials Research Group, Department of Chemical and Biological Engineering, The University of Sheffield, Mappin Street, Sheffield S1 3JD, UK

ARTICLE INFO

Keywords:

Sustainable manufacturing
Porous silica
Kinetics
Reaction engineering
pH

ABSTRACT

The bio-inspired silica (BIS) synthesis is a greener process that operates at ambient and mild pH conditions and produces high-value products with applications in wide areas such as energy, environment, and medicine. In this work, batch and continuous experiments of BIS synthesis were conducted. The experimental data and reaction engineering approach were used to estimate key reaction kinetics relevant to BIS formation over a range of pH. The BIS synthesis was performed in a continuous mode using CSTR and bubble column reactors, resulting in yields comparable to small-scale batch experiments. Using the experimental results and the models, the effects of residence time and feed concentrations were investigated, and optimum conditions were identified. These outcomes will be useful for the scale-up of BIS synthesis, reactor design, and optimization of sustainable manufacturing of high-value silicas.

1. Introduction

Porous silica has various applications in catalysis, adsorption, drug delivery, environmental decontamination, carbon capture, etc. Critical quality attributes (CQAs) of silica in such applications range from particle sizes, surface area, pore sizes, pore volume, degree of aggregation, surface chemistry, etc. [1]. These CQAs depend on the synthesis route, template or surfactant used, solvent properties, pH, and other operating conditions. Silica is synthesized using various methods such as sol-gel method, precipitation method, flame synthesis/pyrolysis, and micro-emulsion method [2–5]. While each of these methods can produce different types/grades of silica, the methods required for producing high-value silicas are generally unsustainable, uneconomical, and/or not scalable [6,7]. On the other hand, bio-inspired synthesis of silicas is relatively greener, flexible to produce silica for wide applications, potentially scalable and cost-effective [8,9]. Bio-silica is naturally produced in many biological organisms (viz. diatoms, sponges and plants) at ambient and mild conditions. Researchers identified that bio-molecules like proteins, peptides and polyamines help in the formation of bio-silica and have explored use of simpler additives to mimic the bio-silica synthesis leading to bio-inspired silica (extensively reviewed in

[8–10]). Brambila et al. [6] have studied the greenness quantitatively for different silica products. Among the different silica synthesis routes, authors concluded that bio-inspired silica is a relatively greener process. Furthermore, bio-inspired silica is operated at ambient conditions and mild pH yet producing materials that are suitable for medium to high value applications viz. catalysis, drug delivery and adsorption. Moreover, the additives in bio-inspired silica can be removed by simple acid elution thus avoiding energy intensive calcination.

Silica formation is a complex reaction, and various researchers have attempted to understand the kinetics particularly using alkoxysilane. Reaction engineering models are useful for reactor design and optimization and there are some literature reports on the kinetics of conventional silica syntheses. For example, Issa and Luyt [12] have reviewed the kinetics of silica formation from sol-gel synthesis using alkoxysilane as a precursor. Silica formation follows the polymerization mechanism, including the hydrolysis of the precursor, followed by a series of condensation reactions followed by the formation/nucleation of a solid phase which grows to form the final structures such as particles, gels, etc. The kinetics of alkoxysilane-based polymerization depends on the concentration of alkoxysilane, water, acid/base, and alcohol [13] and the order of reaction for various species depends on the solvent and

[☆] This article is part of a Special issue entitled: 'ISCRE 28' published in Chemical Engineering Journal.

* Corresponding author.

E-mail address: Vivek.Ranade@ul.ie (V.V. Ranade).

catalysts. Generally, the hydrolysis reaction is first order or pseudo-first order with respect to alkoxy silane while it varies from 0.8 to 4.4 with respect to water. The condensation reaction was second order with respect to organosilane triol [12]. Bari et al. studied the effect of alcohols used as solvents on the kinetics of hydrolysis and condensation with tetraethyl orthosilicate as the starting material [14]. Conversely, in the case of sodium silicate as a starting material, the order of silicic acid condensation was found in the range of 1 to 8 in the literature [15]. The significant variation in the order or reaction is mainly due to the pH of the reaction and catalyst/template which can also affect the reaction mechanism. The rate constant further depends on temperature, pH, and ionic strength. Icopini et al. studied silica oligomerization kinetics and obtained 4th-order dependence for a pH range of 3 to 11 and ionic strength of 0.01 and 0.24 *m* [16]. However, despite the potential for sustainable manufacturing of high-value silica, there are limited reports on the kinetics of bio-inspired silicas [17]. Hence it is essential to develop a kinetic model for better process understanding, reactor design, and scalable process development. In this work, therefore we aim to develop a kinetic model for BIS synthesis and further apply it to continuous reactors. The manuscript is organized as follows: initially, batch and continuous experiments are discussed, followed by kinetic and reactor modelling. Subsequently, experimental, model validation and simulation results are discussed.

2. Experimental section

BIS synthesis typically involves a reaction between sodium silicate, an amine template, and an acid like hydrochloric acid or CO₂ [11]. Different amine templates including a series of ethyleneamines, propyleneamines, natural amines, peptides and polyethyleneimine and polyallylamine are reported in the literature [10]. Furthermore, the amine template can be easily removed after synthesis by acid elution [18,19]. In the present work, we selected pentaethylenehexamine (PEHA) as the bioinspired additive given its fast reaction kinetics and available literature on its use in BIS synthesis. Hydrochloric acid (37%), sodium metasilicate pentahydrate ($\geq 95\%$), and pentaethylenehexamine (technical grade) were procured from Merck Sigma-Aldrich and were used without further purification.

Batch experiments were performed to generate kinetic data and to understand the effect of the mole ratio of hydrochloric acid on the synthesis pH and yield. Continuous experiments were performed in various reactor geometries. The residence time was maintained in the range of 2.5 to 30 min. Stock solutions of sodium silicate pentahydrate (1.0 M), PEHA (0.17 M), and hydrochloric acid (2.0 M) were prepared in deionized (DI) water. The stock solutions were used to prepare feed solutions for all the experiments. All reactions were near isothermal conditions and performed at ambient temperature (18.8 ± 0.6 °C).

2.1. Batch experiments

The initial sodium silicate and PEHA concentrations were 30 mM and 5 mM respectively (i.e. [Si]:[N] = 1) [2] for all experiments unless mentioned otherwise. Batch experiments were performed to study the kinetics and also understand the sensitivity of the HCl mole ratio ([HCl]:[Si]) to the final pH value. The effect of the mole ratio on the final pH is shown in Fig. 1. This experimental data was described by a sigmoidal Eq. (1), which was later used to obtain the desired pH in subsequent experiments. The sigmoidal nature of the Fig. 1 is similar to acid-base titration curve. In the current reaction system, HCl and sodium silicate serve as an acid-base pairs which generate silicic acid. This silicic acid further oligomerizes in presence of PEHA (basic) which also contributes to pH variation in Fig. 1. The Eq. (1) obtained by fitting data can be used to estimate the mole ratio of HCl required for obtaining desired target pH. Experiments were performed in a Corning Gosselin straight plastic container (180 mL). Two different addition protocols were performed in batch experiments. In the first protocol (reaction volume = 20 mL), HCl

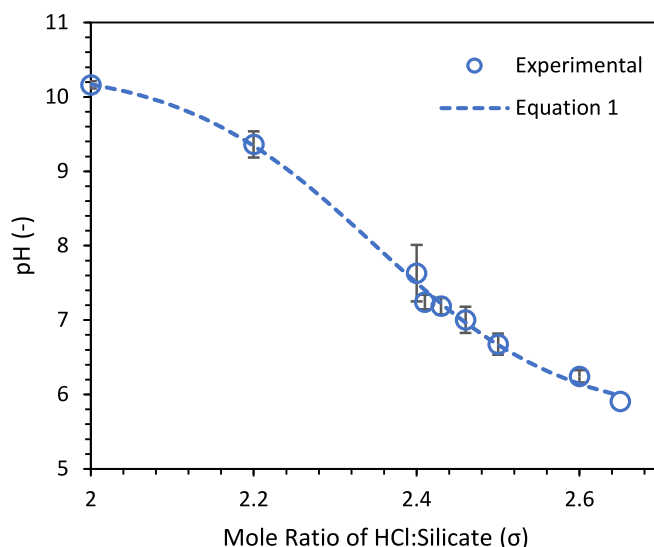


Fig. 1. Relationship between mole ratio (σ) and synthesis pH at the end of batch reaction.

(acid) was added to the basic solution of silicate and PEHA. In contrast, in the second protocol (reaction volume = 100 mL), PEHA (basic) was added to the acidic mixture of silicate and HCl.

Initially, experiments were performed (reaction volume = 20 mL) using the first protocol to measure the concentration profiles. The initial silicate (or monomer) concentration was 50 mM and [Si]:[N] = 1. In this batch experiment silicate and PEHA were premixed in the reactor and HCl was added quickly in one step. Sample collection was started after the HCl addition. For this batch experiment, the initial pH was ~ 12.5 and gradually decreased to ~ 7 at the end of the reaction. The monomer/silicic acid concentration was quantified using the molybdenum method, also known as the molybdate blue method. It involves reacting silicic acid (monomer) with ammonium molybdate to form a yellow silicomolybdic acid complex, which is then reduced to a blue-colored complex and measured spectrophotometrically [2]. Samples were collected for 6 min. Since the analysis of oligomer and polymer requires additional steps and is more complex and time-consuming only the final concentration was measured [2].

In the second protocol (reaction volume = 100 mL), the effect of pH on kinetics and yield was studied. The mole ratio of HCl to sodium silicate was varied from 2.0 to 2.65. Initially, a precalculated volume of HCl (2.0 M) was introduced in a batch reactor (3–3.975 mL depending on the mole ratio) with 50 mL of DI water. To this 3 mL of sodium silicate stock solution (1.0 M) was added using a 10 mL micropipette and then DI water was added to the reactor to make 97 mL of reaction volume. To this mixture, 3 mL of PEHA (0.17 M) stock solution was added rapidly using a 10 mL micropipette. The pH was monitored using a METTLER TOLEDO SevenExcellence S470 Benchtop Meter. After 5 min synthesis, further HCl was added (1.5–1.8 mL) to reduce the reaction pH to ~ 2 and elute the amine additive to purify silica [18]. This pH ~ 2 was reached within 1.5 to 3 min depending on the synthesis endpoint pH. The reaction mixture was stirred at 750 RPM to ensure good mixing and silica suspension. The silica slurry was centrifuged, washed multiple times, and dried at ambient temperature to evaporate water and later in the oven at 60 °C overnight [11].

$$pH = \frac{-4.77}{1 + \exp\left(\frac{\sigma - 2.39}{0.12}\right)} + 10.41 \quad (1)$$

2.2. Continuous experiments

For continuous synthesis, two feed solutions were prepared. Feed

solution-1 was prepared by mixing sodium silicate and HCl solution. The sequence of addition during this feed solution preparation was critical. Initially, 73.5 to 75.6 mL (mole ratio of 2.45 to 2.52) of hydrochloric acid (2.0 M) was diluted with approximately 500 mL of DI water in a volumetric flask. After this dilution, 60 mL sodium silicate stock solution (1.0 M) was added to this in 6 aliquots (10 mL \times 6 times) with periodic shaking of flask. After this addition, the feed solution was further diluted to 1 L with DI water to get the feed concentration of silicate as 60 mM. The feed solution was transferred to a 1 L bottle and the pH was measured. The typical pH of this solution was 1.50 ± 0.02 . Moreover, if this addition sequence is not followed sodium silicate can react with HCl in the feed solution to form a silica gel precipitate (undesired). Feed solution-2 contained 60 mL of PEHA stock solution (0.17 M) diluted with DI water to 1 L to get a feed concentration of 10 mM. The pH of this feed solution was 11.23 ± 0.04 . Fig. 2 shows the schematic of the experimental setup.

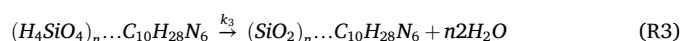
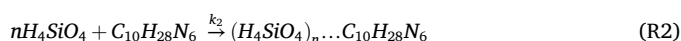
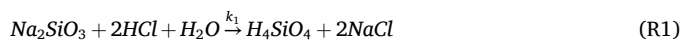
The feed solutions were dosed using a KNF SIMDOS 10 dosing pump (units 3 and 4 in Fig. 2). Different reactors used were a continuous stirred tank reactor (CSTR) (100 mL), helical coil (~62 mL, ID = 4 mm and length = 5 m), a fluidic oscillator (FO) with recirculation loop (49.5 mL), vortex diode (VD) with recirculation loop (42 mL) and bubble column reactor (66 mm ID and 600 mL reactor volume) [11]. Occasionally, a helical coil was used in series with FO and VD. A residence time of 2.5 min to 30 min was maintained in the reactor. The steady-state sample was collected after 4–5 residence times. 600 mL of steady-state sample was collected during each continuous experiment. After sample collection, the silica slurry was acidified to pH ~2 to elute the amine. This acidified slurry was stirred for 5–10 min and later centrifuged, washed, and dried as discussed in the previous section. The samples were analysed to measure surface area as detailed in our previous work [11].

3. Reaction engineering modelling

The main objective of developing a reaction model was to understand the kinetics of the BIS synthesis and use it to predict the yield and find optimum operating conditions. The room temperature synthesis is a novelty of BIS compared to other methods. The long term goal of the work is to develop manufacturing based on this greener process and hence the synthesis was kept at room temperature. Further, the use of high temperature increases operational cost and environment impact. Moreover, it was found that pH is the most critical process parameter affecting yield and particle properties. Hence, in this study we focused on investigating the effect of pH on kinetics.

The BIS synthesis involves simultaneous chemical (conversion of silicic acid to silica) and physical processes (nucleation and further growth of particles by aggregation and agglomeration). Here we are developing a lumped kinetic model (chemical process) involved in the BIS formation. Bio-inspired silica formation is a complex series of reactions involving self-assembly/clustering between the additives and silicate species, hydrolysis of the precursor to form monomer silicic acid, and condensation and polymerization steps via the formation of various intermediate oligomers, finally leading to the formation of silica and their additive-driven aggregation, leading to precipitation of BIS. The early stages reactions (pre-nucleation) and additive-driven aggregation of primary particles control the porosity of BIS (e.g. surface area), which is most important in its intended applications in adsorption and oral drug delivery. Hence, in this work, we focussed on quantifying the influence of pH and residence time on yield by modelling reaction kinetics instead of modelling the particle size distributions. The first reaction in the sequence involves a reaction between sodium silicate (basic) and HCl (acidic) in the aqueous medium (R1). Generally, the acid-base reaction is fast, and the rate of such reactions is controlled by micro-mixing [20]. This reaction is also the fastest in the entire reaction network. However, this reaction takes place in the feed solution since the precursor is acidified before reaching the reactor, hence, modelling

this reaction is not considered here. As such, it was assumed that the sodium silicate completely reacts with acid to form silicic acid in the feed solution. This silicic acid reacts in the presence of the amine additive (PEHA) and undergoes condensation reactions to initially form dimers and trimers, leading to the formation of oligomers. This has been shown in a simplified form as R2¹. PEHA (or amine) is known to have multiple roles in the synthesis viz. catalyst, structure directing agent, growth promoter, template, etc. [10]. Oligomerisation reactions (collectively) are reported as higher-order reactions with orders ranging from 3 to 8 [15–17]. The oligomers further condense/polymerise to form silica as shown in R3. It was assumed that the polymer formation was first order with respect to oligomer concentration. Furthermore, oligomers will grow as a chain and precipitate at a critical chain length; this precipitation is aided by the presence of PEHA, which lowers colloidal stability through surface charge neutralisation [21]. Typically, there will be a distribution of the chain length of the oligomer or polymer [22]. Estimating the exact chain length or the chain distribution of the polymer silica is practically difficult. However, it is known that the lower chain lengths of oligomer viz. dimer and trimer don't precipitate. The oligomer will precipitate at a critical chain length. Here we consider that this average chain length was 'n' for the oligomer and polymer. During the synthesis, depending on the pH, the amine additive, PEHA is protonated (R4), which was assumed to be first order with respect to amine and HCl respectively. The rate constant of this reaction (k_4) was varied from 0 to $0.05 \text{ M}^{-1} \text{ s}^{-1}$, and it had a negligible impact on the yield of BIS. Hence, Reaction 4 was ignored by setting k_4 as zero for estimating other kinetic parameters.



Overall, 5 parameters were fitted: rate constants k_2 and k_3 , order of reaction with respect to monomer (o), parameter for accounting the effect of final synthesis pH (or steady-state pH in the case of continuous experiments) on rate constants (ϕ) and parameter for accounting the effect of pH profile (β) on the BIS synthesis. These parameters were estimated in 3-stages using different experimental datasets. In stage one, k_2 , k_3 , and o were estimated using batch experimental data at pH 7. In the second stage, ϕ was estimated using batch experimental data at various pH values. In the third stage parameter " β " was estimated using continuous experimental data. The system of ODEs was solved in MATLAB 2022a using an *ode15s* solver and kinetic data was fitted using *lsqcurvefit* solver.

In the first stage, monomer concentration data was used to fit rate constants k_2 and order of reaction with respect to monomer (o). After fitting the monomer data, the yield of oligomer and polymer was used to fit the rate constant k_3 . The ratio of k_2/k_3 will remain constant as the temperature is constant for all the experiments. In the second stage, the effect of pH on the rate constants (k_2 and k_3) was estimated. Additional batch experiments were designed at varying HCl molar ratios to achieve a range of pH values. In the batch process, pH gradually reduces to reach the setpoint, while in the case of CSTR, the pH is constant during the synthesis. The final synthesis pH in the batch experiment (or steady state pH in the case of the continuous experiment) was considered for modelling the effect of pH on kinetic parameters. It was assumed that the rate constants (k_2 and k_3) can be related to the pH by Eq. (2). Here pH_{ref}

¹ The dotted line between silicates and PEHA indicates a close association without a chemical bond.

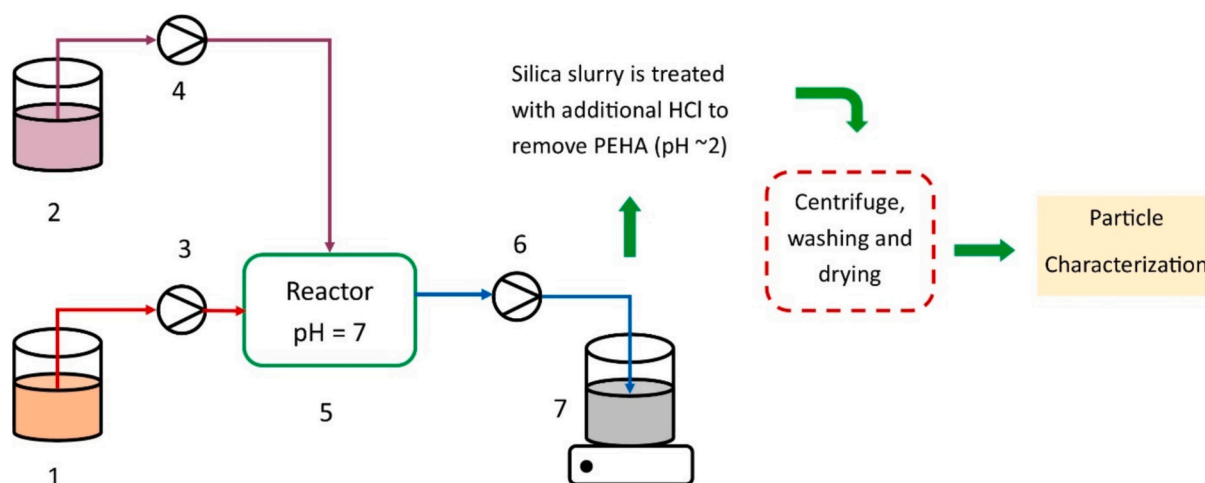


Fig. 2. Continuous synthesis of bio-inspired silica. (1) Feed solution 1, (2) Feed solution 2, (3) and (4) KNF SIMDOS 10 diaphragm pumps, (5) Reactor configuration viz., CSTR, Bubble column, HC, VD with recirculation, FO with recirculation and their combination. (6) Longer Peristaltic pump BT100-3 J-DMD15-13-B for CSTR or bubble column reactor, and (7) Product collection. Feed solution 1: sodium silicate + HCl and feed solution 2: PEHA.

is a reference pH and k_{ref} corresponds to the rate constant value at pH_{ref} . In this work, pH_{ref} was taken as 7.00 for further analysis. The parameter φ was estimated by comparing the isolated yield synthesized at different pH values in the batch reactor. In the third stage, the parameter “ β ” was estimated. The parameter “ β ” accounts for the effect of pH profile during synthesis. In batch synthesis, the pH profile can vary from basic to neutral (or acidic) or from acidic to neutral (or basic) depending on the nature of the addition of the reagents. On the contrary, for CSTR the synthesis pH will be constant, and the kinetic parameters estimated will be free from any effect of the pH profile. Hence kinetic parameters were estimated using continuous experiments at various pH values and the parameter “ β ” was set as 1 for the continuous experiments. The parameter “ β ” was further estimated by back-calculating it from the rate constants at pH_{ref} for previously discussed batch experiments.

$$\frac{k}{k_{ref}} = \beta \left(\frac{pH}{pH_{ref}} \right)^{\varphi} \quad (2)$$

Eq. (3) is the generalized mole balance equation for CSTR and batch reactors. The flow rates q_1 and q_2 correspond to feed solution 1 (silicate-HCl mixture) and feed solution 2 (PEHA). The flowrates (q_1 , q_2 , and q_T) are set to zero for batch reactors. Table 1 shows the rate expression/source terms for all the species considered here.

$$V \frac{dC_k}{dt} = q_1 C_{k1in} + q_2 C_{k2in} - q_T C_k + V R_k \quad (3)$$

For estimating kinetic parameters, a combined CSTR and semi-batch model was used, and the rate constant was fitted manually by comparing the isolated yield. The CSTR and semi-batch model resembles the actual CSTR reactor and product collection respectively. The predicted outlet concentrations of CSTR model were used as inlet conditions for semi-batch model, and the semi-batch model was integrated till the product collection time. The product collection time was calculated based on the total flowrate in the actual experiment to achieve final collected volume of 600 mL. The product collection volume (600 mL) was constant for all

experiments (irrespective of residence time in the CSTR). Solving the CSTR and semi-batch reactor models in series is representative of the actual experiment operated at a steady state of CSTR. Since, the reaction and product collection happen at same temperature and pH, the same kinetic parameters were used for both the models. It should be further noted that simulations ‘with product collection’ involved both CSTR and semi-batch model while simulations ‘without product collection’ involved only CSTR model.

4. Results and discussion

4.1. Estimation of reaction kinetics

In batch experiments, silicic acid concentration was measured over the reaction duration, and the concentrations of the polymer and oligomers were measured only at the end of the reaction. These experimental data were considered for the estimation of kinetic parameters. Batch reaction equations were solved for monomer (silicic acid), and PEHA to estimate kinetic parameters k_2 and order of reaction with respect to monomer (α). The chain length (n) was kept at 20 while estimating the above parameters. It was observed that the overall reaction of 5th order with respect to monomer gives the best fit (see Fig. S1 in the Supplementary Information).

After estimating the above kinetic parameters (k_2 and α), equations for the batch reactor were solved for all the species, and experimental data of the monomer, oligomer, and polymer were used to estimate the rate constant k_3 . The estimated kinetic parameters are shown in Table 2. After estimating the order of reaction and kinetic parameters, the effect of chain length (n) on the predicted conversion and yield was studied. Different n values were tested ($n = 20, 30$, and 40). Since the source of the monomer consumption (Table 1) has the term “ $n \times k_2$ ”, the product “ $n \times k_2$ ” was held constant (1.30×10^7) during fitting. The fitting was good for all “ n ” values. Table S1 in the Supporting Information shows the conversion of monomers and yields of different species for different fitted parameters (see Table S1 of the supplementary information). There is a slight variation in conversion and yield as the rate of

Table 1
Rate expression for different species.

Species	Symbol	Rate
Silicic acid (monomer)	M	$-nk_2 C_M^{\alpha} C_A$
PEHA	A	$-k_2 C_M^{\alpha} C_A$
Oligomer	O	$k_2 C_M^{\alpha} C_A - k_3 C_O$
Silica (polymer)	P	$k_3 C_O$

Table 2
Rate constants for BIS synthesis (at pH = 7.02).

Rate constant [unit]	Value
$k_2 [M^{-5} s^{-1}]$ for $n = 20$	6.49×10^5
$k_3 [s^{-1}]$	0.0039
Order of reaction with respect to monomer (α)	5

consumption of PEHA only depends on k_2 and is independent of n . Since the fitting was good for all “ n ” values, $n = 20$ was considered. Fig. 3 shows the kinetic data and model comparison for the batch experiment. Additional details about the fitted parameters are given in the Supporting Information (see Table S2).

It should be noted that in this experiment the starting pH in the reactor was basic (~ 12.5) and reached neutral pH towards the end of the reaction. The concentration profile of monomer reaches a near constant value at ~ 0.01 M due to higher order of reaction (5th order with respect to monomer and 1st order with respect to PEHA). Higher order reactions usually don't go to completion as the rate of reaction is significantly reduced at lower concentrations (towards the end of reaction). This is in agreement with the literature reports [15–17]. Though the silica formation may exhibit reversibility theoretically, the lower solubility of silica in water drives the reaction in forward direction. Hence the backward reaction was not considered here.

After estimating the kinetic parameters at pH ~ 7 (Fig. 3), additional batch experiments were performed for various HCl molar ratios (2.0 to 2.65) to understand the effect of pH on silica yield and kinetics (Section 2.1). It should be noted that this method involves adding PEHA to the mixture of silicate-HCl, unlike the previous protocol where HCl is added to the mixture of silicate-PEHA [2]. This addition protocol was selected as it provides an advantage when translating to a continuous process discussed in the later section. No significant precipitation was observed during the reaction timeframe for the mole ratio of 2.6 and 2.65 corresponding to final pH values of 6.24 and 5.90 respectively. Moreover, silica gel-like material was formed at a lower mole ratio of 2.0 (pH = 10.16) instead of bio-inspired silica. Both results are consistent with the literature and the known mechanisms of the effects of pH on silica formation [13,23]. Hence the HCl molar ratio range of 2.2 to 2.5 was considered to understand the impact of pH on BIS yield and kinetics. The pH of the precursor-acid mixture before adding PEHA was in the range of ~ 1.9 to ~ 3.4 for the mole ratio of 2.5 to 2.2 respectively. Fig. 4 (A) shows the isolated yield for the batch experiments at various pH values measured at 5 min. Fig. 4 (B) shows the corresponding surface area of silica particle. All the batch experiments were planned for 5 min, however, during quenching it takes ~ 2 min to reach the pH ~ 2 value. Thus, effective reaction time was considered during kinetic parameter estimation and simulation.

As discussed earlier, the ratio k_2/k_3 will be constant as the temperature is constant. Initially, kinetic parameters (k_2 and k_3) were fitted to match the isolated yield for pH 7.05 ± 0.15 experiment. Further, Eq. (2)

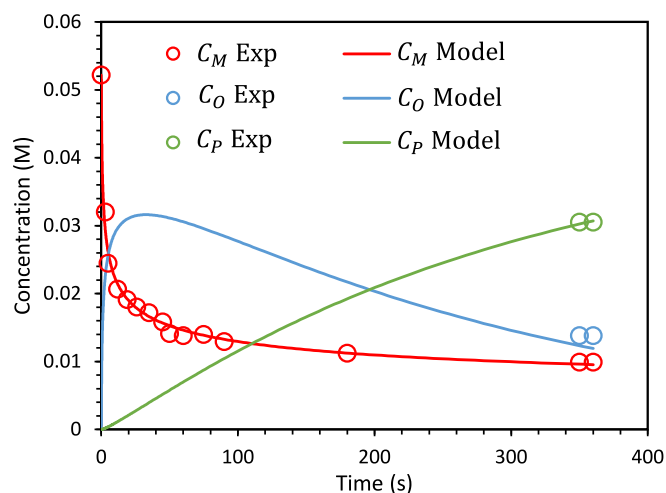


Fig. 3. Prediction of monomer, oligomer, and polymer concentrations using estimated kinetic parameters. The actual concentration of oligomer and polymer is multiplied by chain length, $n = 20$ during plotting for better visualization. The final pH at the end of synthesis was 7.02.

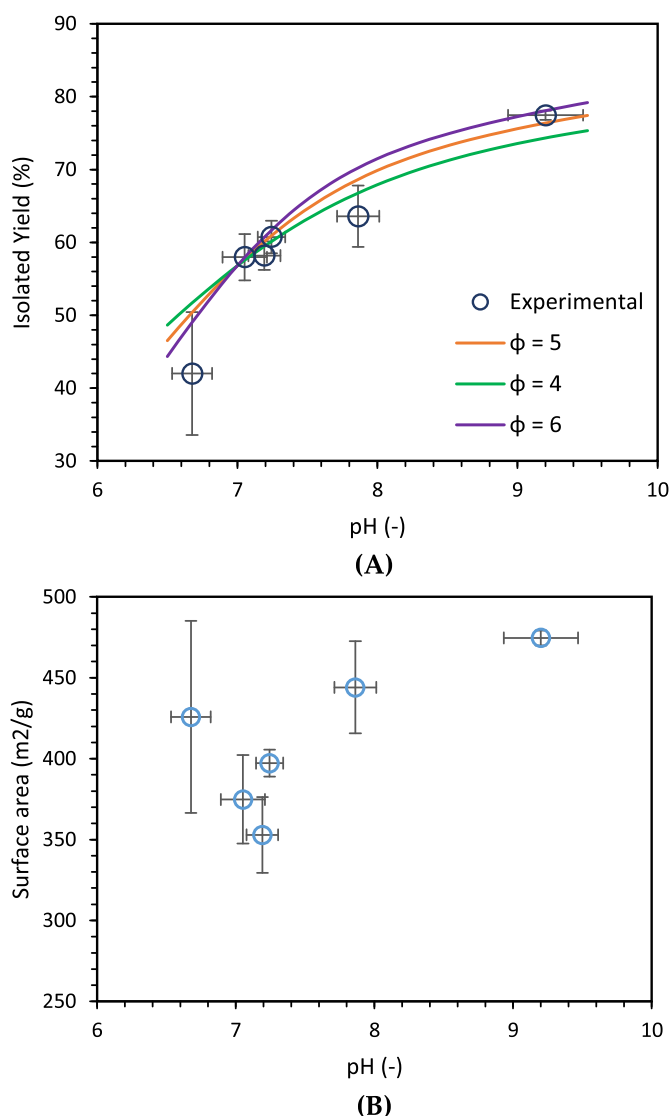


Fig. 4. Effect of pH on (A) Yield of BIS and (B) BET surface area in Batch Reactor for mole ratio of 2.2 to 2.5.

was used to fit the parameter ϕ by comparing the isolated yield with the predicted yield and using the above estimated kinetic parameters (k_{2ref} and k_{3ref} estimated at pH_{ref}) as reference points. It can be seen from Fig. 4(A) that $\phi = 6$ gives a better fit. Furthermore, $\phi = 6$ also has a relatively lower sum of squares error (see Fig. S2 in the SI). Hence $\phi = 6$ was selected for further analysis. It should be noted that the estimated rate constants for the batch experiments are lumped with “ β ” which was estimated later. Additional details about the fitted kinetic parameters and associated errors in yield prediction are given in the Supporting Information (see section S2).

Interestingly, the kinetic parameters estimated at near ~ 7 pH in the case of Figs. 3 and 4 (A) differ by $\sim 26\%$ (or by factor 1.26). This can be attributed to different pH profiles and addition methods. Fig. 4 (A) involves the addition of basic PEHA solution into the acidified silicate precursor solution (pH in the reactor changes from 1.96 to ~ 7). On the contrary, Fig. 3 represents the results from the synthesis where the acid was added to the basic mixture of silica and PEHA (pH in the reactor changes from ~ 12.5 to ~ 7). This results in different lumped rate constant values despite the same final pH. Furthermore, isolated yield data (Fig. 6A) from continuous experiments (CSTR) were used to fit the kinetic parameters k_2 and k_3 . Since the pH is constant in the CSTR, the kinetic parameters estimated are not lumped by the effect of the pH

profile, unlike batch experiments. Hence the parameter β was set as one for the case of CSTR and was used to calculate the β for batch experiments discussed previously by comparing the estimated rate constants ($k_{2\text{ref}}$ and $k_{3\text{ref}}$) at pH_{ref} . Fig. 5 shows the effect of the final pH and the pH profile (or synthesis addition method) on the estimation of lumped rate constants (k_2 and k_3).

4.2. Application of model to simulate continuous experiments

Continuous synthesis experiments were performed to generate experimental data for validating the model and evaluating the effects of reactor geometries. Initially, we conducted continuous experiments using the traditional continuous method [11]. This method involves using a silicate-PEHA mixture as the first feed solution and HCl as the second feed solution. However, with this approach, it was difficult to maintain the desired pH of ~ 7 owing to small variations in volumetric ratios or feed concentrations, caused by pump fluctuations or using new stock solutions. While syringe pumps have excellent accuracy and precision in dosing on average, they may cause instantaneous fluctuations and are generally unsuitable for long operation times or milli-scale reactors. To address this challenge, we developed a relatively robust

method with a modified HCl addition strategy, where the HCl and silicate were premixed in the feed solution (Section 2.2). This ensures that the mole ratio of HCl and silicate is always constant and not sensitive to pump fluctuations. Eq. (1) was used to get the desired HCl mole ratio for the target pH value during feed solution preparation. This strategy was supplemented with predesigned batch experiments for every new stock solution preparation (see Fig. 1).

Initially, Continuous experiments were performed in a CSTR, helical coil (HC), fluidic oscillator (FO), and vortex diode with helical coil in series (VD + HC) with a residence time of 5 min. It was observed that there was significant fouling in the helical coil, fluidic oscillator, and vortex diode. The fouling resulted in a significant accumulation of silica particles lowering the yield and causing operational issues. There was also occasional clogging in the fluidic oscillator at a higher initial silicate concentration (60 mM). The isolated yields for the helical coil, fluidic oscillator (FO), and vortex diode with the helical coil in series (VD + HC) were 35%, 30%, and 16% respectively. On the contrary, there was reasonably low fouling in the CSTR. Fouling in the case of the CSTR mostly occurred on the outlet tube, reactor walls, and the pH probe. However, this did not affect the isolated yield significantly ($\sim 52\%$). Hence, we decided to use CSTR for further model validation. Given the constant steady-state pH in CSTR, the kinetic parameters estimated from continuous synthesis were not lumped with the pH profile. Hence the parameter β was set as one for the continuous synthesis (Eq. 2). Furthermore, the rate constants estimated at $\text{pH} \sim 7$ were used as reference values to calculate β for batch experiments (see Fig. 5 and Eq. 2).

Continuous syntheses were performed at different residence times and pH values in the CSTR. Fig. 6 (A) shows the comparison of the isolated yield with the predicted yield. Note that the predicted yield considers both residence and collection time for calculations. Since the synthesis and product collection also happen at ambient conditions, the reaction will continue to happen during the product collection time. This was accounted for when comparing the predicted and isolated yield of silica by modelling product collection as a semi-batch process. Ignoring the semi-batch model will not provide the true representation of the current experimental system. The semi-batch model may be ignored if continuous separation is employed or if reaction is quenched in-line. However, in the present case batch centrifugation was employed making semi-batch modelling essential. The outlet concentration of the CSTR model was used as input or initial conditions for the semi-batch model and was simulated till 600 mL final volume with the product collection time ranging from 15 to 60 min depending on the flowrates. The model was able to accurately predict the yield as can be seen from the comparison with the experimental data in Fig. 6 (A). Small variations can be attributed to fouling and losses during downstream purification.

The surface area of BIS ranged from 292 m^2/g to 579 m^2/g for various pH and residence times investigated. It can be seen that a higher surface area was obtained at lower pH. This trend is in agreement with the published literature [24]. More details about BIS characterization and its comparison with different silica products can be found in the literature [6–8,11,24].

The trade-off between yield and surface area as a function of pH makes operating at $\text{pH} \sim 7$ desirable. Furthermore, the developed kinetic model can be used to find the optimum residence time for synthesis at lower pH to get both higher yield and higher surface area respectively.

Fig. 7 (A) shows the isolated yield and productivity for continuous synthesis for various pH and residence times and the trend is similar to that seen for batch experiments (Fig. 4). In the case of continuous experiments, the final isolated yield not only depends in the reactor residence time but also on pH, product collection time, and operational factors like fouling and work-up which lead to yield losses. Recovering silica particle from a dilute reaction mixture (~ 30 mM) and low yield experiments (residence time = 2.5 min) is challenging. Furthermore, fouling is stochastic phenomenon affected by factors such as reactant

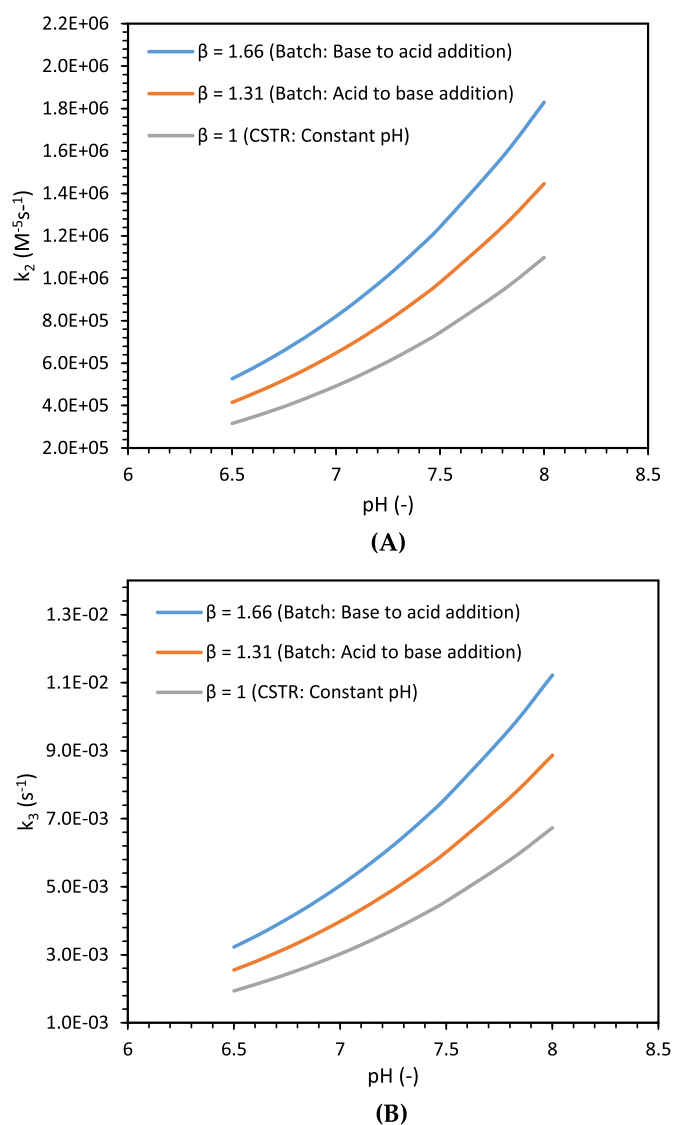
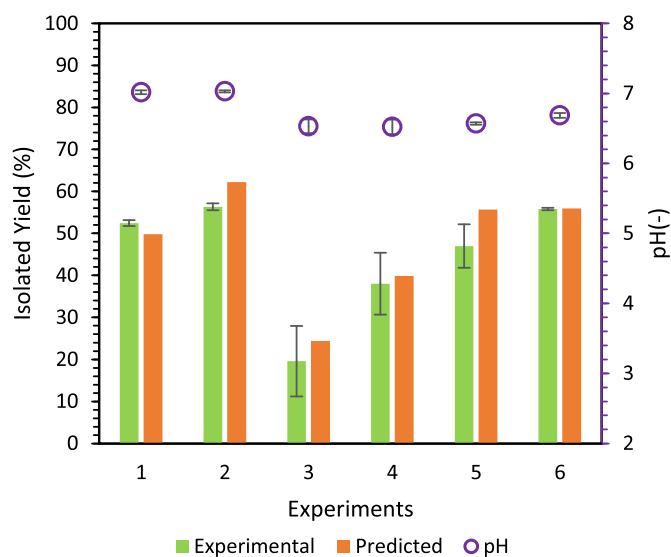
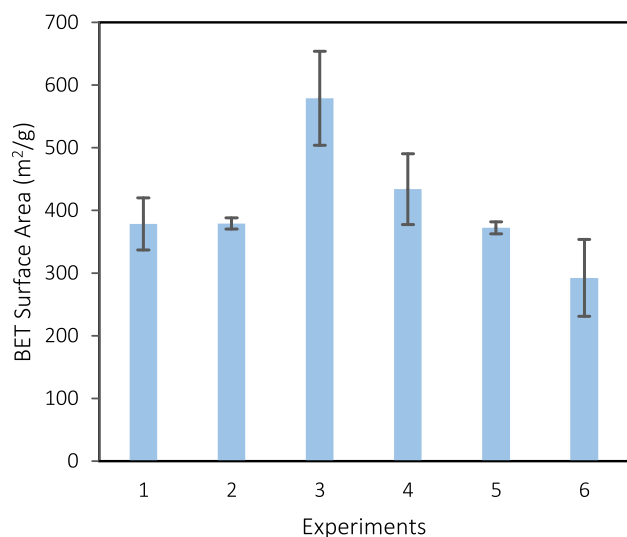


Fig. 5. Estimated rate constants and the impact of pH profile modelled using the fitting parameter β . Here $\phi = 6$, $k_{2\text{ref}} = 3.32 \times 10^5 \text{ M}^{-5} \text{ s}^{-1}$ and $k_{3\text{ref}} = 2.03 \times 10^{-3} \text{ s}^{-1}$ (A) k_2 and (B) k_3 .



(A)

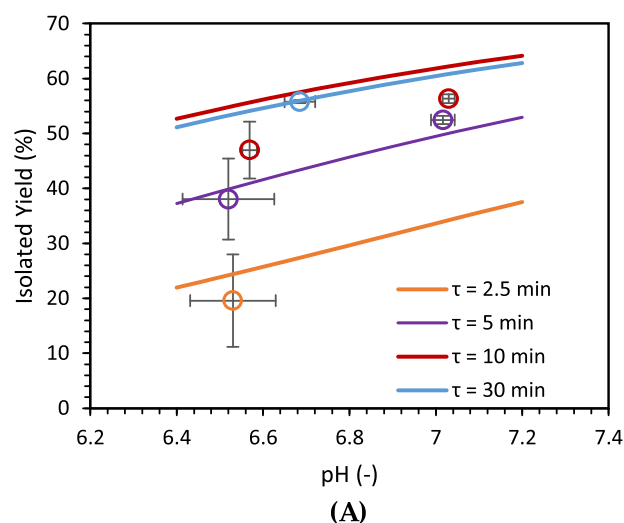


(B)

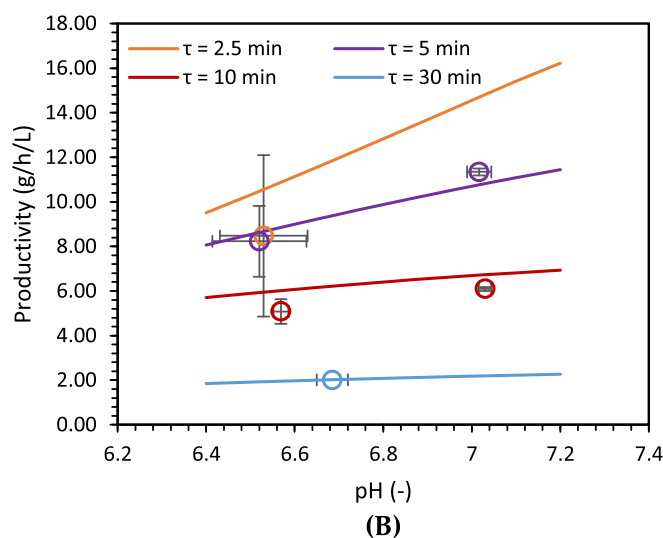
Fig. 6. (A) Comparison of isolated yield and predicted yield in the CSTR and (B) BET surface area of pH 2 silica samples (1) $\tau = 5$ min, $\text{pH} = 7.02 \pm 0.03$, (2) $\tau = 10$ min, $\text{pH} = 7.03 \pm 0.01$, (3) $\tau = 2.5$ min, $\text{pH} = 6.53 \pm 0.1$, (4) $\tau = 5$ min, $\text{pH} = 6.52 \pm 0.1$, and (5) $\tau = 10$ min, $\text{pH} = 6.57 \pm 0.02$, and (6) $\tau = 30$ min, $\text{pH} = 6.69 \pm 0.04$. (1)–(5) represents CSTR (reactor volume = 100 mL) and (6) represents bubble column reactor (reactor volume = 600 mL with N_2 bubbling at 1 LPM for mixing).

flow rates, reactor scale, pH, and mechanical vibrations.

These combined effects on yield can be explained by comparing the experiments conducted at 10-minute and 30-minute residence times. In the 10-minute experiment, a reactor volume of 100 mL was used with a total flow rate of 10 mL/min and a product collection time of 60 min. The lower flow rate and longer operation time led to increased fouling and yield loss. To minimize fouling and extended operation, the 30-minute experiment was conducted using a larger reactor (600 mL) with a higher total flow rate of 20 mL/min and a shorter product collection time of 30 min. As a result, the effective reaction durations (residence time plus collection time) were comparable in both experiments (70 min vs. 60 min, respectively). Although the isolated yields were similar, fouling was significantly higher in the 10-minute residence time experiment. This resulted in higher error between predicted and experimental yield for 10 min residence time. It can be seen that the



(A)



(B)

Fig. 7. Effect of steady-state pH on (A) Isolated yield and (B) Productivity. The symbols and lines indicate experimental and simulated results respectively. The colour code indicates residence time.

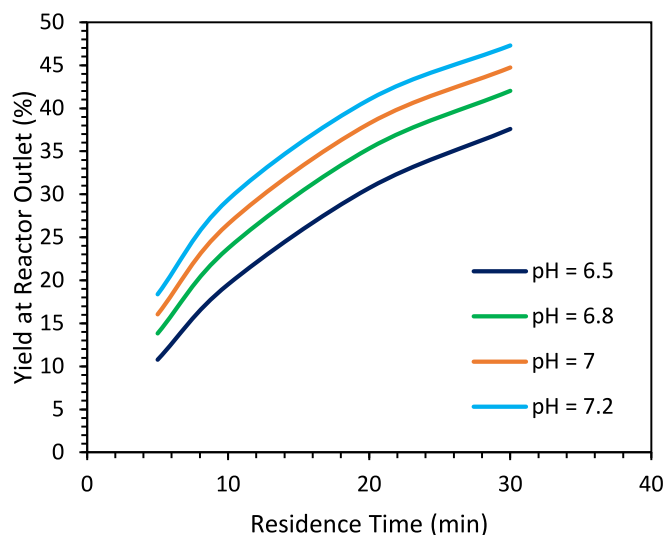


Fig. 8. Reactor outlet yield simulated at various pH and residence times (Initial concentration of Monomer and PEHA were 30 mM and 5 mM respectively). Note that product collection time is not considered here.

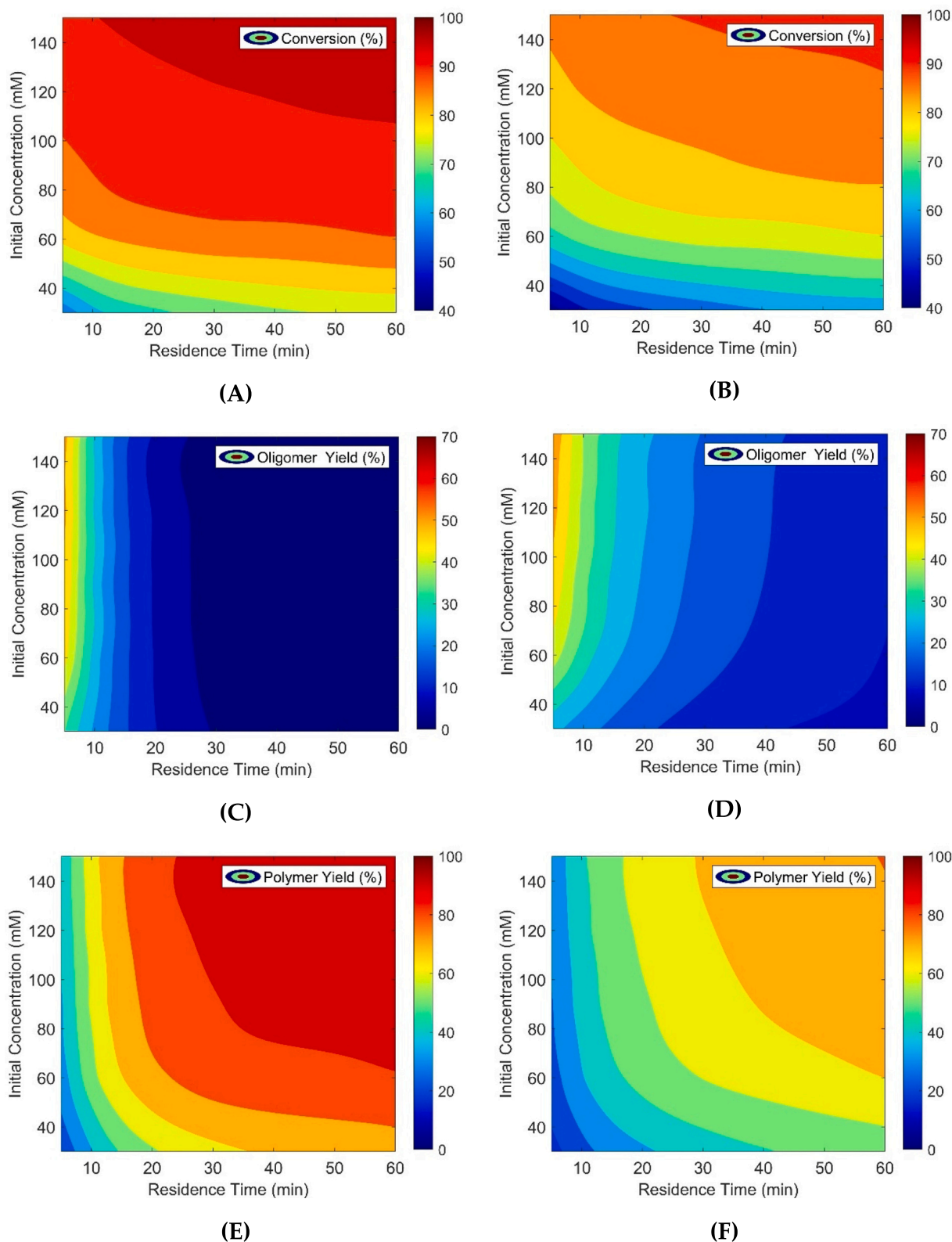


Fig. 9. Design space for optimization using PFR and CSTR models. PFR models: (A), (C), and (E) and CSTR models: (B), (D), and (F) represent monomer conversion, oligomer yield, and polymer yield respectively. Product collection was not included in simulations.

yield for a residence time of 10 min was only marginally higher (by $\sim 1.5\%$) than a residence time of 30 min, perhaps indicating that there is no added benefit from running the reaction beyond 10 min at this experimental scale. These yields were converted to productivity (amount of BIS produced per volume per time) and a maximum

productivity of 11.34 g/L/h was obtained for CSTR with 5 min residence time and pH of ~ 7 .

Additional simulations were performed to quantify the yield at the reactor outlet conditions without product collection (Fig. 8). This result may be useful for optimizing the process if the silica slurry is directly

processed continuously without any collection time (or negligible holding time). Initial concentration, residence time, and pH (or HCl mole ratio) can be optimized to get the desired yield and surface area.

4.3. Optimization and design space

After validating the model, we used the model to quantitatively understand influence of backmixing in the reactor. Tubular reactors with appropriate configurations like helical coil or coiled flow inverter may approach ideal plug flow reactor (PFR) while vigorously stirred vessel may approach fully backmixed reactor (CSTR). Tubular reactors will give higher (than CSTR) conversion and yield for any positive order reaction. However, due to better solid handling ability, CSTR may be a practical choice for the reactor. Multiple CSTRs in series may also be used to achieve performance close to PFR without problems due to solids handling. With this background, we used the developed model to simulate performance of PFR and CSTR. We selected an initial silicate concentration and residence time as 30 to 150 mM and 5 to 60 min. Rate constants at pH 7 were considered. The monomer conversion is an overall 6th-order reaction with 5th-order with respect to monomer and 1st-order with respect to PEHA. The simulated results are shown in Fig. 9.

The rate of higher-order reaction is sensitive to the initial concentration. This can be seen in Fig. 9 (A) and (B) respectively. There is a significant increase in conversion from 30 mM to 80 mM, which is consistent with previously reported small-scale batch results [23,25], and the conversion becomes relatively constant above 80 mM. For lower concentrations, below 40 mM, conversion is slightly sensitive towards residence time, however, it reaches a constant value after ~30 min. For higher concentrations, the conversion is almost independent of the residence time. A lower yield of the oligomer and higher monomer conversion is desired to maximise the polymer (silica) yield. Fig. 9 (C) and (D) show that the oligomer yield is independent of the initial concentration of the monomer as the reaction is first order with respect to the monomer. The oligomer yield decreased significantly from 5 min to 25 min residence time (for PFR) and from 5 min to ~30 min (for CSTR) and reached a plateau. This residence time range ensures that the oligomer is converted to the desired polymer. Fig. 9 (E) and (F) show the polymer (silica) yield for PFR and CSTR respectively. The rate of polymer formation depends on both the monomer and oligomer consumption. Hence it is dependent on both initial concentration and residence time. While high silicate concentrations seem to favour higher yields, at higher concentrations of the silicate-HCl feed solution ($\gg 100$ mM), the higher viscosity of the mixture can cause mixing/handling issues and is likely to result in premature gelation [25]. Furthermore, after 30 min residence time, there was no significant improvement seen in the yield, however, yield from CSTR was lower compared to the PFR.

Higher concentrations ($\gg 100$ mM) may be feasible in general, if silicate and HCl are directly mixed in the reactor instead of preparing the feed solution separately. This may avoid undesired premature precipitation of silica gel as discussed previously. Additionally, despite relatively lower concentrations, the bio-inspired silica synthesis have shown promising properties and cost advantages compared to other silica synthesis routes [6,8].

Since CSTRs were found to be practically easier for BIS synthesis, in order to explore if CSTRs in series could be better, we performed simulations of 5 CSTR in series and 30 min total residence time with initial silicate concentration ranging from 30 mM to 90 mM. Fig. 10 shows the yield comparison of PFR and CSTR in series. Additional results on the simulated conversion and yield of oligomer and polymer are presented in the Supporting Information (Fig. S4). The residence time is 30 min for the five CSTR-in-series case and thus, the individual residence time for each CSTRs is 6 min. As expected, there is a significant improvement in the conversion and yield after 3 CSTRs and the performance approaches PFR for five CSTR in series.

An alternative to CSTRs is a bubble column reactor where inert gas

like air or nitrogen can be used for mixing. We evaluated the feasibility of BIS synthesis in a bubble column reactor (see Fig. 6 (A), entry 6). The bubble column had a lower aspect ratio (<3), resembling a CSTR. The ratio of residence time and mixing time for both these reactors were of the order 10^2 suggesting that both the reactors have homogeneously mixed slurry. Therefore, for the BIS synthesis and modelling point of view, there are no significant differences in the performance of CSTR and bubble column reactors. However, bubble column reactor is relatively easy to construct and operate and does not require an agitator as mixing can be achieved by gas bubbling. Overall CSTR and bubble column reactors both give comparable results and are scalable.

In summary, the developed kinetic model successfully captures the effect of pH and residence time on yield in spite of the practical experimental challenges like fouling and yield losses during work-up. While, some deviations in experiments are observed due to pH sensitivity and fouling, model still provides valuable insights for researchers and engineers working on continuous synthesis of bio-inspired silica and similar nanoparticle systems.

5. Conclusions

In this work, we have developed a kinetic model and continuous process for bio-inspired silica using PEHA as an amine template and hydrochloric acid. Kinetic parameters were estimated at various pH values using batch and continuous experimental data. A power law correlation was developed to predict the rate constants for various synthesis methods and pH values. The developed correlation can be used to estimate the rate constants for transient pH experiments in batch reactors (acid-to-base addition and vice versa) and constant pH experiments in the case of CSTR. The kinetic model was validated using continuous reactors viz. CSTR and bubble column reactor. A maximum yield of over 55% was obtained in the CSTR and bubble column reactor with relatively low fouling. The maximum productivity of 11.34 g/L/h was obtained in CSTR for 5 min residence time. The surface area of BIS particles in continuous experiments was 292 m^2/g to 579 m^2/g for the pH range of 6.5 to 7. The surface area of BIS particles in batch experiments was 352 m^2/g to 474 m^2/g for the pH range of 6.6 to 9.2. Simulations were performed for a range of residence times (5–60 min) and feed concentrations (30–150 mM) to generate design space for finding optimum conditions using PFR and CSTR models. The presented kinetic

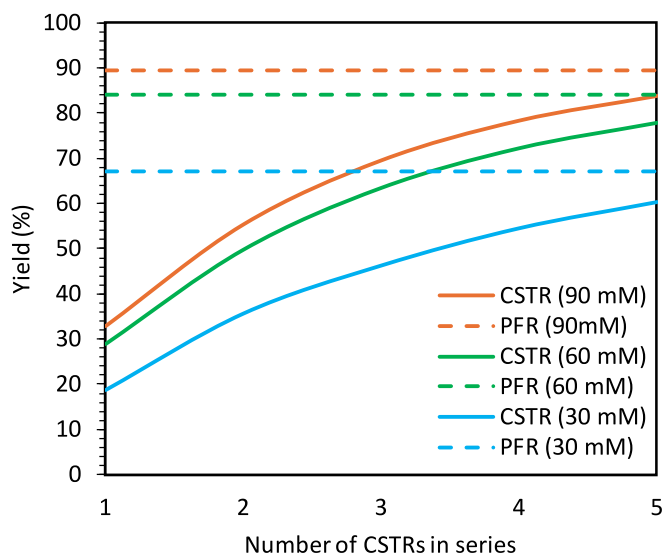


Fig. 10. Yield comparison of PFR and 5-CSTR in series for different concentrations. The residence time of PFR and 5-CSTR in series is 30 min. Simulations are without product collection.

model and results will be useful for further reactor design and developing scalable processes for bio-inspired silica production.

Nomenclature

C_M	concentration of silicic acid or monomer (M)
C_A	concentration of PEHA (M)
C_O	concentration of Oligomer (M)
C_P	concentration of Polymer (M)
C_k	concentration of species 'k' (M)
C_{k1in}	concentration of species 'k' (M)
k_1	rate constant for Monomer formation ($M^{-1} s^{-1}$)
k_2	rate constant for Oligomer formation ($M^{-5} s^{-1}$)
k_{2ref}	reference rate constant for k_2 at pH_{ref} ($M^{-5} s^{-1}$)
k_3	rate constant for Polymer formation (s^{-1})
k_{3ref}	reference rate constant for k_3 at pH_{ref} (s^{-1})
k_4	rate constant for PEHA-salt formation ($M^{-1} s^{-1}$)
n	stoichiometric coefficient or chain length
o	order of reaction with respect to monomer
pH_{ref}	reference pH = 7
Q_1	feed 1 flowrate (L/s)
Q_2	feed 2 flowrate (L/s)
Q_T	total or outlet flowrate (L/s)
R_k	rate of reaction for k^{th} species (Ms^{-1})
t	time (s)
σ	mole ratio of HCl with respect to sodium silicate
φ	exponent parameter for the effect of pH on rate constants
β	kinetic parameter for the effect of pH profile

CRediT authorship contribution statement

Chinmay A. Shukla: Writing – original draft, Methodology, Investigation, Formal analysis, Data curation. **Roja P. Moghadam:** Investigation, Formal analysis, Data curation. **Amber Keegan:** Investigation, Formal analysis, Data curation. **Siddharth V. Patwardhan:** Writing – review & editing, Supervision, Project administration, Funding acquisition. **Vivek V. Ranade:** Writing – review & editing, Supervision, Resources, Project administration, Funding acquisition, Conceptualization.

Declaration of competing interest

The authors declare that they have no known competing financial interests or personal relationships that could have appeared to influence the work reported in this paper.

Acknowledgements

The authors express their sincere gratitude for the financial support provided by Science Foundation Ireland (SFI, 21/EPSC/3766) and the Engineering and Physical Sciences Research Council (EPSRC, EP/V051458/1 and EP/R025983/1). The authors thank Amol Ganjare for developing an Arduino-based pH sensor for measurement.

Appendix A. Supplementary data

Supplementary data to this article can be found online at <https://doi.org/10.1016/j.cej.2025.165010>.

Data availability

Data will be made available on request.

References

- [1] A.A. Nayl, A.I. Abd-Elhamid, A.A. Aly, S. Bräse, Recent progress in the applications of silica-based nanoparticles, *RSC Adv.* 12 (22) (2022) 13706–13726, <https://doi.org/10.1039/D2RA01587K>.
- [2] J.R.H. Manning, E. Routoula, S.V. Patwardhan, Preparation of functional silica using a bioinspired method, *JoVE* 138 (2018) e57730, <https://doi.org/10.3791/57730>.
- [3] D. Bokov, A. Turki Jalil, S. Chupradit, W. Suksatan, M. Javed Ansari, I.H. Shewael, G.H. Valiev, E. Kianfar, Nanomaterial by sol-gel method: synthesis and application, *Adv. Mater. Sci. Eng.* 2021 (1) (2021) 5102014, <https://doi.org/10.1155/2021/5102014>.
- [4] K.S. Finnie, J.R. Bartlett, C.J.A. Barbé, L. Kong, Formation of silica nanoparticles in microemulsions, *Langmuir* 23 (6) (2007) 3017–3024, <https://doi.org/10.1021/la0624283>.
- [5] E.D.E.R. Hyde, A. Seyfaee, F. Neville, R. Moreno-Atanasio, Colloidal silica particle synthesis and future industrial manufacturing pathways: a review, *Ind. Eng. Chem. Res.* 55 (33) (2016) 8891–8913, <https://doi.org/10.1021/acs.iecr.6b01839>.
- [6] C. Brambila, P. Boyd, A. Keegan, P. Sharma, C. Vetter, E. Ponnusamy, S. V. Patwardhan, A comparison of environmental impact of various silicas using a green chemistry evaluator, *ACS Sustain. Chem. Eng.* 10 (16) (2022) 5288–5298, <https://doi.org/10.1021/acssuschemeng.2c00519>.
- [7] C. Drummond, R. McCann, S.V. Patwardhan, A feasibility study of the biologically inspired green manufacturing of precipitated silica, *Chem. Eng. J.* 244 (2014) 483–492, <https://doi.org/10.1016/j.cej.2014.01.071>.
- [8] R. Pilling, S.V. Patwardhan, Recent advances in enabling green manufacture of functional nanomaterials: a case study of bioinspired silica, *ACS Sustain. Chem. Eng.* 10 (37) (2022) 12048–12064, <https://doi.org/10.1021/acssuschemeng.2c02204>.
- [9] S.V. Patwardhan, J.R.H. Manning, M. Chiacchia, Bioinspired synthesis as a potential green method for the preparation of nanomaterials: opportunities and challenges, *Curr. Opin. Green Sustain. Chem.* 12 (2018) 110–116, <https://doi.org/10.1016/j.cogsc.2018.08.004>.
- [10] S.V. Patwardhan, S.S. Staniland, *Green Nanomaterials, From Bioinspired Synthesis to Sustainable Manufacturing of Inorganic Nanomaterials*, IOP Publishing, 2019.
- [11] C.A. Shukla, R.P. Moghadam, S.V. Patwardhan, V.V. Ranade, Feasibility and advantages of continuous synthesis of bioinspired silica using CO₂ as an acidifying agent, *ACS Sustain. Chem. Eng.* 12 (27) (2024) 10260–10268, <https://doi.org/10.1021/acssuschemeng.4c03101>.
- [12] A.A. Issa, A.S. Luyt, Kinetics of alkoxysilanes and organoalkoxysilanes polymerization: a review, *Polymers* 11 (3) (2019) 537, <https://doi.org/10.3390/polym11030537>.
- [13] C.J. Brinker, G.W. Scherer, *Sol-gel Science*, Academic Press, San Diego, 1990, <https://doi.org/10.1016/B978-0-08-057103-4.50006-4>.
- [14] A.H. Bari, R.B. Jundale, A.A. Kulkarni, Understanding the role of solvent properties on reaction kinetics for synthesis of silica nanoparticles, *Chem. Eng. J.* 398 (2020) 125427, <https://doi.org/10.1016/j.cej.2020.125427>.
- [15] S. Scott, I.M. Galeczka, I. Gunnarsson, S. Arnórsson, A. Stefánsson, Silica polymerization and nanocolloid nucleation and growth kinetics in aqueous solutions, *Geochim. Cosmochim. Acta* 371 (2024) 78–94, <https://doi.org/10.1016/j.gca.2024.02.017>.
- [16] G.A. Icopini, S.L. Brantley, P.J. Heaney, Kinetics of silica oligomerization and nanocolloid formation as a function of pH and ionic strength at 25°C, *Geochim. Cosmochim. Acta* 69 (2) (2005) 293–303, <https://doi.org/10.1016/j.gca.2004.06.038>.
- [17] D.J. Belton, O. Deschaume, S.V. Patwardhan, C.C. Perry, A solution study of silica condensation and speciation with relevance to in vitro investigations of biosilicification, *J. Phys. Chem. B* 114 (31) (2010) 9947–9955, <https://doi.org/10.1021/jp101347q>.
- [18] J.R.H. Manning, T.W.S. Yip, A. Centi, M. Jorge, S.V. Patwardhan, An eco-friendly, tunable and scalable method for producing porous functional nanomaterials designed using molecular interactions, *ChemSusChem* 10 (8) (2017) 1683–1691, <https://doi.org/10.1002/cssc.201700027>.
- [19] S.V. Patwardhan, J.R.H. Manning, *Silica Synthesis*, 2017. WO2017037460.
- [20] J.R. Bourne, Mixing and the selectivity of chemical reactions, *Org. Process. Res. Dev.* 7 (4) (2003) 471–508, <https://doi.org/10.1021/op020074q>.
- [21] D.J. Belton, S.V. Patwardhan, C.C. Perry, Spermine, spermidine and their analogues generate tailored silicas, *J. Mater. Chem.* 15 (43) (2005) 4629–4638, <https://doi.org/10.1039/B509683A>.
- [22] R.K. Iler, *The Chemistry of Silica, Solubility, Polymerization, Colloid and Surface Properties, and Biochemistry* 866, 1979.
- [23] L. Dewulf, M. Chiacchia, A.S. Yeardeley, R.A. Milton, S.F. Brown, S.V. Patwardhan, Designing bioinspired green nanosilicas using statistical and machine learning approaches, *Mol. Syst. Des. Eng.* 6 (4) (2021) 293–307, <https://doi.org/10.1039/D0ME00167H>.
- [24] J.R.H. Manning, C. Brambila, S.V. Patwardhan, Unified mechanistic interpretation of amine-assisted silica synthesis methods to enable design of more complex materials, *Mol. Syst. Des. Eng.* 6 (3) (2021) 170–196, <https://doi.org/10.1039/D0ME00131G>.
- [25] J.R.H. Manning, C. Brambila, K. Rishi, G. Beaucage, G.L. Davies, S.V. Patwardhan, Quality-by-design approach to process intensification of bioinspired silica synthesis, *ACS Sustain. Chem. Eng.* 12 (12) (2024) 4900–4911, <https://doi.org/10.1021/acssuschemeng.3c07624>.